

# Exact nonequilibrium dynamics of finite-temperature Tonks-Girardeau gases

Y. Y. Atas,<sup>1</sup> D. M. Gangardt,<sup>2</sup> I. Bouchoule,<sup>3</sup> and K. V. Kheruntsyan<sup>1</sup>

<sup>1</sup>*University of Queensland, School of Mathematics and Physics, Brisbane, Queensland 4072, Australia*

<sup>2</sup>*School of Physics and Astronomy, University of Birmingham, Edgbaston, Birmingham, B15 2TT, UK*

<sup>3</sup>*Laboratoire Charles Fabry, Institut d'Optique, CNRS, Université Paris Sud 11,*

*2 Avenue Augustin Fresnel, F-91127 Palaiseau Cedex, France*

(Dated: June 14, 2022)

Describing finite-temperature nonequilibrium dynamics of interacting many-particle systems is a notoriously challenging problem in quantum many-body physics. Here we provide an exact solution to this problem for a system of strongly interacting bosons in one dimension in the Tonks-Girardeau regime of infinitely strong repulsive interactions. Using the Fredholm determinant approach and the Bose-Fermi mapping we show how the problem can be reduced to a single-particle basis, wherein the finite-temperature effects enter the solution via an effective “dressing” of the single-particle wavefunctions by the Fermi-Dirac occupation factors. We demonstrate the utility of our approach and its computational efficiency in two nontrivial out-of-equilibrium scenarios: collective breathing mode oscillations in a harmonic trap and collisional dynamics in the Newton's cradle setting involving real-time evolution in a periodic Bragg potential.

*Introduction.*—Out-of-equilibrium phenomena are as prevalent in natural and engineered systems as equilibrium ones. Despite this, our understanding of nonequilibrium states of matter is far inferior to the understanding of equilibrium states governed by the broadly applicable foundational principles of statistical mechanics. In recent years, ultracold quantum gases have emerged as a platform-of-choice for studying nonequilibrium dynamics of interacting quantum many-body systems [1–6]. This is due to the fact that such gases represent nearly-ideal and highly controllable realisations of various models of many-body theory in which such dynamics can be accessed on observable time scales. A particularly active area here concerned the study of quantum quenches and mechanisms of relaxation in 1D Bose gases [7–11] (see also [4, 12–17] and references therein), which, in the uniform limit, can be well approximated by the integrable Lieb-Liniger model [18] with delta-function pairwise interactions between the particles.

The limit of infinitely strong repulsive interactions in the Lieb-Liniger model corresponds to a 1D gas of impenetrable (hard-core) bosons, or the Tonks-Girardeau (TG) gas. The strong interactions required for realizing the TG gas have been achieved in ultracold atom experiments in highly anisotropic traps [7, 19–21], and its spectacular dynamics in a quantum Newton's cradle setting were observed in Ref. [7]. The particle impenetrability in the TG gas allows one to map the problem of many interacting bosons to an ideal (noninteracting) gas of fermions [22]. Remarkably, the Bose-Fermi mapping and hence the exact integrability of the model works not only in the uniform limit but also for inhomogeneous systems [23–25], which enables accurate tests of theory against experiments that are typically performed in harmonic traps. Despite this, and despite the relatively long history behind the model, theoretical studies of TG gases have so far been limited to either zero- and finite-temperature *equilibrium* properties or *zero-temperature* dynamics [24, 26–31]. *Finite-temperature dynamics*, on the other hand, has not been studied yet, which is important for accurate comparisons with experiments that

are realised at nonzero temperatures.

In this work, we develop an exact finite-temperature dynamical theory of the TG gas applicable to arbitrary external potentials. More specifically, we propose a computationally efficient method for calculating the dynamics of single-particle density matrix and the corresponding momentum distribution of the gas. The method is based on the Fredholm determinant approach and the Bose-Fermi mapping, which allows one to solve the dynamical many-body problem in terms of the dynamics of single-particle quantities. This is similar to the zero-temperature approach of Ref. [27], except that we take into account finite-temperature effects. This results in an effective “dressing” of the single-particle wavefunctions by the square roots of Fermi-Dirac occupation factors. Our formalism is equally applicable to finite-temperature equilibrium calculations, in which case it offers significant computational advantages over the previously used approaches based on Lenard's formula [32–34]. For harmonically trapped systems, the efficiency of our approach is further unveiled by utilising known analytic integrals and recurrent relations between Hermite polynomials.

*Examples of evolution of the TG gas from a thermal state.*—As an immediate application and illustration of the broad applicability of our approach, we use it to analyse two paradigmatic problems of current experimental and theoretical interest: (a) collective breathing-mode oscillations of a finite-temperature TG gas in a harmonic trap, and (b) collisional dynamics in the Newton's cradle setting which involves real-time evolution in a periodic Bragg potential.

For this we consider a 1D gas of  $N$  bosons of mass  $m$ , interacting via repulsive two-body delta-function potential and confined by a time-dependent one-body trapping potential  $V(x, t)$  described by the Hamiltonian

$$\hat{H} = \sum_{j=1}^N \left[ -\frac{\hbar^2}{2m} \frac{\partial^2}{\partial x_j^2} + V(x_j, t) \right] + g \sum_{j < l} \delta(x_j - x_l). \quad (1)$$

where  $g > 0$  is the interaction strength. The infinitely strong contact interactions ( $g \rightarrow \infty$ ) correspond to the TG gas of

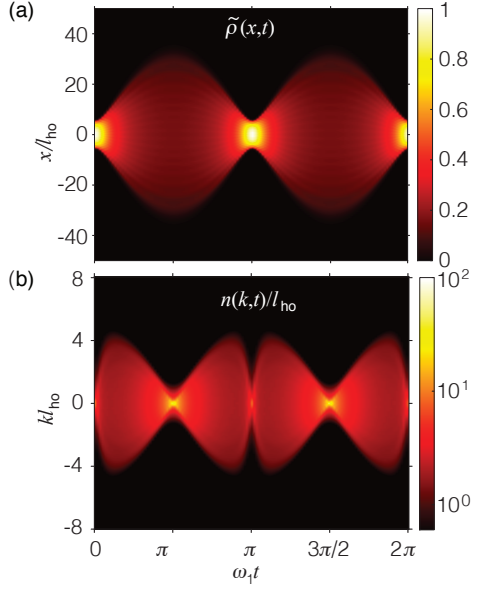


FIG. 1. (Color online) Breathing-mode dynamics of the TG gas following a confinement quench. (a) Real-space density  $\tilde{\rho}(x, t) \equiv \rho(x, t)/\rho(0, 0)$  and (b) momentum distribution,  $n(k, t)/l_{ho}$  (where  $l_{ho} = \sqrt{\hbar/m\omega_0}$  is the harmonic oscillator length) as functions of the dimensionless time  $\omega_1 t$ , for  $N = 16$  particles, quench strength  $\epsilon = 35$ , and dimensionless initial temperature  $\theta_0 \equiv k_B T_0/N\hbar\omega_0 = 0.01$ .

impenetrable bosons [18, 22]. In this limit the interactions are replaced by the hard-core constraints and the quantum many-body problem can be solved exactly.

Our goal is to study the real-time evolution of the one-body density matrix

$$\rho(x, y; t) = \frac{1}{\mathcal{Z}} \sum_{N, \alpha} e^{\beta(\mu N - E_\alpha)} \int dx_2 \dots dx_N \times \Psi_\alpha(x, x_2, \dots, x_N; t) \Psi_\alpha^*(y, x_2, \dots, x_N; t). \quad (2)$$

Here,  $\mathcal{Z} = \sum_{N, \alpha} e^{\beta(\mu N - E_\alpha)}$  is the grand-canonical partition function,  $\beta \equiv 1/k_B T_0$ ,  $\mu$  is the initial chemical potential, and  $\Psi_\alpha(x_1, \dots, x_N; t)$  is the  $N$ -body wavefunction evolved according to the Schrödinger equation from the initial wavefunction  $\Psi_\alpha(x_1, \dots, x_N; 0)$ .

At time  $t = 0$ , Eq. (2) describes the initial thermal equilibriums state of the system in the trapping potential  $V(x, 0)$  at temperature  $T_0$ . The density matrix allows one to calculate important observables, such as the real-space density  $\rho(x, t) = \rho(x, x; t)$  and the momentum distribution  $n(k, t) = \int dx dy e^{-ik(x-y)} \rho(x, y; t)$  of the gas.

For the first application of our approach to collective oscillations, we consider a TG gas in thermal equilibrium in a harmonic potential  $V(x, 0) = m\omega_0^2 x^2/2$  with the initial frequency  $\omega_0$ . To invoke the breathing-mode oscillations we use a confinement quench in which at  $t = 0$  the trapping frequency is instantaneously changed from the pre-quench value  $\omega_0$  to a new value  $\omega_1$ ; we characterise the quench strength by the dimensionless parameter  $\epsilon = \omega_0^2/\omega_1^2 - 1$ . Figure 1

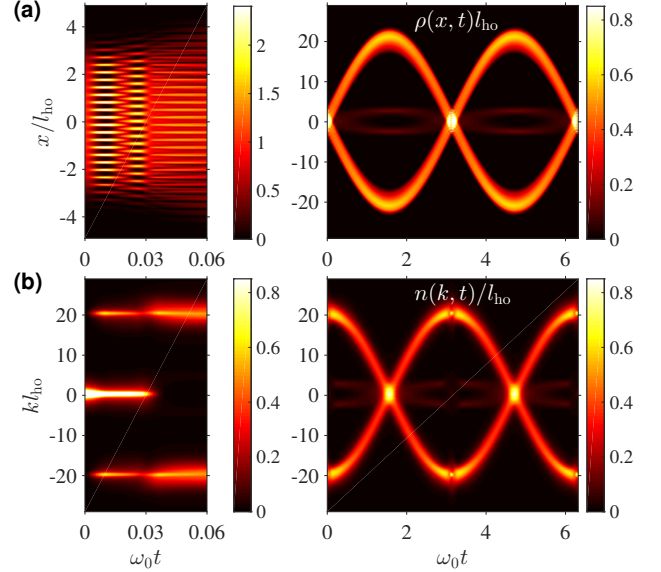


FIG. 2. (Color online) Dynamics of the TG gas in the Newton's cradle setting. In (a) we show the evolution of the real-space density,  $\rho(x, t)l_{ho}$  as a function of the dimensionless time  $\tau = \omega_0 t$ ; the left panel is the magnified view into the time window containing the Bragg pulse sequence, whereas the right panel shows the full time window including post-Bragg periodic oscillations in the purely harmonic potential. In (b) we show the respective momentum distribution,  $n(k, t)/l_{ho}$ . In this example,  $\theta_0 = 0.5$ ,  $N = 5$ , and  $k_0 l_{ho} = 10$ . The overall Bragg pulse consists of two square pulses of duration  $\tau_B = \pi/4\sqrt{2}\omega_B$  each, during which  $\Omega(t) = 2\sqrt{2}\omega_B$  (with  $\omega_B \equiv \hbar k_0^2/2m$ ), interrupted by a waiting interval of duration  $\tau_{\text{wait}} = \pi/4\omega_B$ , during which  $\Omega(t) = 0$  [37]; the overall duration of this double-Bragg pulse is  $\tau_{B, \text{total}} = 0.0379$ , after which the population is nearly completely transferred from the zero-centered momentum component into the  $\pm 2\hbar k_0$  components.

shows the evolution of the density profile  $\rho(x, t)$  and the momentum distribution  $n(k, t)$  after a strong quench ( $\epsilon = 35$ ), for  $N = 16$  particles and a dimensionless initial temperature of  $\theta_0 \equiv k_B T_0/N\hbar\omega_0 = 0.01$ . As we show below using the scaling solutions of Eq. (8), the dynamics of  $\rho(x, t)$  consists of self-similar broadening/narrowing cycles occurring at the fundamental breathing-mode frequency of  $\omega_B = 2\omega_1$ . In contrast, the momentum distribution displays periodic broadening/narrowing cycles that occur at *twice* the rate of the oscillations of the *in situ* density profile. Unlike the breathing-mode oscillations of an ideal Fermi gas, the momentum distribution of the TG gas becomes narrow not only at the outer turning points of the classical harmonic oscillator motion, when the *in situ* density profile is the broadest (corresponding to time instances of  $\omega_1 t = \pi/2 + \pi l$ , with  $l = 1, 2, \dots$ ), but also at  $\omega_1 t = \pi l$  when the gas is maximally compressed. We refer to these points as the *inner* turning points, which serve as a manifestation of a collective many-body bounce effect due to the increased thermodynamic pressure of the gas that acts as a potential barrier. This phenomenon is similar to frequency doubling observed recently in a weakly-interacting quasicondensate regime [11, 35] and is further explored in Ref. [36].

As a second application of our approach, we analyse the dynamics of a finite-temperature TG gas in the Newton's cradle setting [7]. In this example, the initial atomic cloud in thermal equilibrium at temperature  $\theta_0 = 0.5$  is subjected to a sequence of laser induced Bragg pulses optimised to split the atomic wavepacket into two counter-propagating halves corresponding to  $\pm 2\hbar k_0$  diffraction orders of Bragg scattering [37]. This is modelled by a periodic lattice potential  $V_B(x, t) = \Omega(t) \cos(2k_0 x)$  of an amplitude  $\Omega(t)$ , superimposed on top of the initial harmonic potential of frequency  $\omega_0$ . Unlike the (short pulse) Kapitza-Dirac regime of Bragg scattering analyzed in Ref. [31], we operate in the (long pulse) Bragg regime of the Newton's cradle experiment [7] wherein the interatomic interactions during the Bragg pulse are automatically taken into account, rather than neglected. The resulting collisional dynamics of the gas in the underlying harmonic potential is shown in Fig. 2 and will be further analyzed elsewhere [38].

We now outline the derivation of the time-dependent one-body density matrix of the TG gas used in the above examples.

*Fredholm determinant approach to one-body density matrix and its evolution.*—The reduction of the many-body dynamical problem of a TG gas to a single particle evolution relies on the existence of a Bose-Fermi mapping [22, 24, 25, 39],

$$\Psi_\alpha(x_1, \dots, x_N; t) = A(x_1, \dots, x_N) \Psi_\alpha^F(x_1, \dots, x_N; t), \quad (3)$$

between the many-body wavefunctions  $\Psi_\alpha$  of *interacting* (hard-core) bosons and those of *free* fermions,  $\Psi_\alpha^F$ , where the function  $A(x_1, \dots, x_N) = \prod_{1 \leq j < i \leq N} \text{sgn}(x_i - x_j)$  ensures the symmetrization of the bosonic wavefunctions.

The fermionic many-body wavefunctions can be constructed as Slater determinants  $\Psi_\alpha^F(x_1, \dots, x_N; t) = \det_{i,j=1}^N [\phi_{\alpha_i}(x_j, t)] / \sqrt{N!}$  of single-particle wavefunctions  $\phi_{\alpha_i}(x, t)$  evolving according to the Schrödinger equation, with the initial wavefunctions  $\phi_{\alpha_i}(x, 0)$  being the eigenstates of the trapping potential  $V(x, 0)$ , with eigenenergies  $E_{\alpha_i}$  such that  $E_\alpha = \sum_{i=1}^N E_{\alpha_i}$  and the index  $\alpha = \{\alpha_1, \dots, \alpha_N\}$  representing the set of single-particle quantum numbers  $\alpha_i$  that may occur.

As was shown by Lenard in Ref. [32], the Bose-Fermi mapping allows one to express the one-body density matrix of the TG gas, Eq. (2), in terms of the fermionic one-body density matrix  $\rho_F(x, y; t) = \sum_{i=0}^{\infty} f_i \phi_i(x; t) \phi_i^*(y; t)$ , which is a sum of products of single-particle wavefunctions weighted by the Fermi-Dirac occupation factors  $f_i = [e^{(E_i - \mu)/k_B T_0} + 1]^{-1}$ . The resulting expression for  $\rho(x, y; t)$  is an infinite sum of multiple integrals of products of  $\rho_F(x, y; t)$  at different points [40]. Here, we instead follow the approach of Refs. [41, 42], which identified an alternative and more compact form of Lenard's formula, given by

$$\rho(x, y; t) = \det \left( 1 - 2\hat{K}(t) \right) R(x, y; t), \quad (4)$$

i.e., by a product of a Fredholm determinant and the associated resolvent operator  $R(x, y; t)$  of the integral operator  $\hat{K}$ , whose action on an arbitrary function  $g(r)$  is

given by  $(\hat{K}g)(w) = \int_x^y K(w, r; t)g(r)dr$ , with the Kernel  $K(w, r; t) \equiv \rho_F(w, r; t)$ . The resolvent operator  $R(x, y; t)$  satisfies the following integral equation [42],

$$R(u, v; t) - 2 \int_x^y K(u, r; t)R(r, v; t)dr = K(u, v; t). \quad (5)$$

Here, we have assumed  $y \geq x$  without loss of generality and suppressed, for notational simplicity, the dependence of  $R$  on the integration limits as the final results that we are interested in only depend on the values of  $R$  at  $u = x$  and  $v = y$ .

As we show in Ref. [40], Eq. (4) can be reduced to a simple double sum, which does not contain multiple integrals or sign-alternating terms present in Lenard's formula,

$$\rho(x, y; t) = \sum_{i,j=0}^{\infty} \sqrt{f_i} \phi_i(x, t) Q_{ij}(x, y; t) \sqrt{f_j} \phi_j^*(y, t), \quad (6)$$

where  $Q_{ij}$  are the matrix elements of the operator  $\mathbf{Q}(x, y; t) = (\mathbf{P}^{-1})^\top \det \mathbf{P}$ , with

$$P_{ij}(x, y; t) = \delta_{ij} - 2 \text{sgn}(y - x) \sqrt{f_i f_j} \int_x^y dx' \phi_i(x', t) \phi_j^*(x', t). \quad (7)$$

Equations (6) and (7) are the main results of this paper, representing a compact and computationally practical recipe for calculating the time-dependent one-body density matrix of the TG gas. They reduce the problem of finding  $\rho(x, y; t)$  to solving the time-dependent Schrödinger equation for the single-particle orbitals  $\phi_j(x, t)$  and calculating the matrix elements  $P_{ij}(x, y; t)$ . At time  $t = 0$ , Eq. (6) describes the initial equilibrium one-body density matrix; in its present form it offers a more efficient and accurate way of calculating  $\rho(x, y; 0)$  compared to the previous approaches [32, 33].

At zero temperature Eqs. (6)–(7) reduce to the results of Ref. [27] as the Fermi-Dirac distribution function in this case is given by a step function equal to 1 for orbitals with  $i \leq N - 1$ , or 0 otherwise. At nonzero temperature the orbital wavefunctions, as our results show, become effectively “dressed” by the square roots of the respective Fermi-Dirac occupation factors, ensuring, e.g., that the correct real-space density  $\rho(x, t) \equiv \rho(x, x; t) = \sum_{i=0}^{\infty} f_i |\phi_i(x, t)|^2$  is recovered.

*Dynamics in a harmonic trap and evaluation of the overlap matrix  $\mathbf{P}$ .*—The calculation of the one-body density matrix  $\rho(x, y; t)$ , Eq. (6), requires, in general, the evaluation of the overlap matrix elements  $P_{ij}(x, y; t)$ , Eq. (7), between the time-evolved wavefunctions  $\phi_j(x, t)$ , starting from the initial single-particle wavefunctions  $\phi_j(x, 0)$ . For the special case of evolution in a time-dependent harmonic trap,  $V(x, t) = m\omega(t)^2 x^2/2$ , the wavefunctions  $\phi_j(x, 0)$  are given by the well-known Hermite-Gauss orbitals, whereas the evolution under single-particle Schrödinger equation can be solved using a scaling transformation [26, 43], which in turn leads to

$$\rho(x, y; t) = \frac{1}{\lambda} \rho_0(x/\lambda, y/\lambda) e^{im\lambda(x^2 - y^2)/2\hbar\lambda}, \quad (8)$$

where  $\rho_0(x, y) = \rho(x, y; 0)$  is the initial one-body density matrix. The scaling parameter  $\lambda(t)$  is determined from the

solution to the second-order ordinary differential equation (ODE),  $\ddot{\lambda} = -\omega(t)^2 \lambda + \omega_0^2/\lambda^3$ , with the initial conditions  $\lambda(0) = 1$ , and  $\dot{\lambda}(0) = 0$ . For the quench of the trapping frequency considered above, this ODE acquires the form of the Ermakov-Pinney equation,  $\ddot{\lambda} = -\omega_1^2 \lambda + \omega_0^2/\lambda^3$ , with the solution  $\lambda(t) = [1 + \epsilon \sin^2(\omega_1 t)]^{1/2}$ ,

The scaling solution (8) simplifies enormously the calculation of  $\rho(x, y; t)$  as Eq. (6) is used only once—for calculating the *initial* equilibrium density matrix  $\rho_0(x, y)$  of a harmonically trapped TG gas. In this case, the elements of the overlap matrix  $P_{ij}(x, y; 0)$  are computed for the harmonic oscillator eigenstates,  $\phi_j(x) = e^{-x^2/2l_{ho}^2} H_j(x/l_{ho})/(\pi^{1/4} \sqrt{2^j j! l_{ho}})$ , where  $H_j(\xi)$  is the Hermite polynomial of degree  $j$  ( $j = 0, 1, 2, \dots$ ), and  $l_{ho} = \sqrt{\hbar/m\omega_0}$  is the harmonic oscillator length. One then computes the determinant of the initial overlap matrix  $\mathbf{P}$  and inverts it in order to evaluate the matrix elements  $Q_{ij}(x, y, 0)$  appearing in Eq. (6).

In order to describe higher temperature samples and larger total number of atoms  $N$  with this seemingly straightforward procedure, one needs to incorporate increasingly higher orbital wavefunctions in the double sum in Eq. (6). This, in turn, requires the evaluation of the overlap integrals between highly excited states in Eq. (7). (For example, for our highest temperature and highest  $N$  samples, we used harmonic-oscillator excited states of up to  $j = 400$ .) As the highly excited states are fast oscillating functions in position space, brute-force numerical integration will result in computational difficulties.

To overcome these difficulties, we instead develop and compute the overlap matrix elements using an alternative approach. Namely, for the off-diagonal elements,  $P_{jk}(x, y; 0)$  ( $j \neq k$ ), we resort to a known analytic formula for the harmonic oscillator eigenstates, given in the form of the following indefinite integral [44]

$$\int \varphi_j(\xi) \varphi_k^*(\xi) d\xi = \frac{e^{-\xi^2}}{2(k-j)\sqrt{2^{j+k}\pi} j! k!} \times [H_{j+1}(\xi) H_k(\xi) - H_j(\xi) H_{k+1}(\xi)], \quad (9)$$

where  $\xi \equiv x/l_{ho}$  and  $\varphi_j(\xi) \equiv \sqrt{l_{ho}} \phi_j(x)$ . This formula is much simpler to use, especially at higher temperatures and larger  $N$ , than the one based on a finite series of confluent hypergeometric functions used in Ref. [33].

For the diagonal elements  $P_{jj}(x, y; 0)$ , no similar formula exists to the best of our knowledge, however, we find that these elements can be computed efficiently using the following recursive method. We define a sequence of functions  $\{M_j(\xi)\}_{j=0,1,\dots}$  containing the desired diagonal matrix elements in the form of indefinite integrals,

$$M_j(\xi) = \frac{\sqrt{\pi}}{2} \text{erf}(\xi) - \frac{1}{2^j j!} \int e^{-\xi^2} H_j^2(\xi) d\xi, \quad (10)$$

where  $\text{erf}(\xi)$  is the error function and  $M_0(\xi) = 0$ . Using the well-known recurrence relation for the Hermite polynomials, we obtain

$$M_{j+1}(\xi) = M_j(\xi) + \frac{e^{-\xi^2}}{2^{j+1}(j+1)!} H_j(\xi) H_{j+1}(\xi). \quad (11)$$

Equations (9)–(11) thus allow for an efficient computation of all (diagonal and off-diagonal) matrix elements of  $P_{ij}(x, y; 0)$  without performing explicit numerical integration of products of harmonic oscillator wavefunctions.

In conclusion, we have developed an exact finite-temperature dynamical theory of the Tonks-Girardeau gas applicable to arbitrary initial temperatures and trapping potentials, including arbitrary variations of the trapping potentials with time. The approach relies on the Fredholm determinant representation and the Bose-Fermi mapping, allowing one to reduce the problem of many-body evolution to a single-particle basis. For harmonically trapped gases, the approach further benefits from analytic scaling solutions for the single-particle wavefunctions, while for arbitrary trapping potentials the wavefunctions should be evolved numerically according to the single-particle Schrödinger equation. Our results open the way to systematic studies of nonequilibrium dynamics of this paradigmatic strongly interacting many-body system; the examples illustrated here concerned the breathing-mode oscillations and the Newton's cradle setup, however, other nonequilibrium scenarios can be easily considered, such as periodic driving, collisions in anharmonic traps, and formation of quantum shock waves, to name a few.

The authors acknowledge fruitful discussions with Y. Castin, E. Bogomolny, and O. Giraud. Y. Y. A. thanks R. J. Lewis-Swan for the introduction to the XMDS software package used in the numerical simulations of the single-particle Schrödinger equation. I. B. acknowledges support by the Centre de Compétences Nanosciences Île-de-France. K. V. K. acknowledges support by the Australian Research Council Discovery Project Grant DP140101763.

---

- [1] I. Bloch, J. Dalibard, and W. Zwerger, *Rev. Mod. Phys.* **80**, 885 (2008).
- [2] M. A. Cazalilla and M. Rigol, *New Journal of Physics* **12**, 055006 (2010).
- [3] A. Polkovnikov, K. Sengupta, A. Silva, and M. Vengalattore, *Rev. Mod. Phys.* **83**, 863 (2011).
- [4] M. A. Cazalilla, R. Citro, T. Giamarchi, E. Orignac, and M. Rigol, *Rev. Mod. Phys.* **83**, 1405 (2011).
- [5] A. Lamacraft and J. Moore, in *Ultracold bosonic and fermionic gases*, Vol. 5 (Contemporary Concepts in Condensed Matter Science), Eds. K. Levin, A. L. Fetter, and D. M. Stamper-Kurn (Elsevier, The Netherlands, 2012).
- [6] J. Eisert, M. Friesdorf, and C. Gogolin, *Nature Physics* **11**, 124 (2015).
- [7] T. Kinoshita, T. Wenger, and D. S. Weiss, *Nature* **440**, 900 (2006).
- [8] S. Hofferberth, I. Lesanovsky, B. Fischer, T. Schumm, and J. Schmiedmayer, *Nature* **449**, 324 (2007).
- [9] S. Trotzky, Y.-A. Chen, A. Flesch, I. P. McCulloch, U. Schollwöck, J. Eisert, and I. Bloch, *Nature Physics* **8**, 325 (2012).
- [10] M. Gring, M. Kuhnert, T. Langen, T. Kitagawa, B. Rauer, M. Schreitl, I. Mazets, D. A. Smith, E. Demler, and J. Schmiedmayer, *Science* **337**, 1318 (2012).

- [11] B. Fang, G. Carleo, A. Johnson, and I. Bouchoule, *Phys. Rev. Lett.* **113**, 035301 (2014).
- [12] J.-S. Caux and R. M. Konik, *Phys. Rev. Lett.* **109**, 175301 (2012).
- [13] D. Iyer and N. Andrei, *Phys. Rev. Lett.* **109**, 115304 (2012); D. Iyer, H. Guan, and N. Andrei, *Phys. Rev. A* **87**, 053628 (2013).
- [14] M. Kormos, A. Shashi, Y.-Z. Chou, J.-S. Caux, and A. Imam-bekov, *Phys. Rev. B* **88**, 205131 (2013).
- [15] J. De Nardis, B. Wouters, M. Brockmann, and J.-S. Caux, *Phys. Rev. A* **89**, 033601 (2014).
- [16] J. C. Zill, T. M. Wright, K. V. Kheruntsyan, T. Gasenzer, and M. J. Davis, *Phys. Rev. A* **91**, 023611 (2015); *New Journal of Physics* **18**, 045010 (2016).
- [17] L. Piroli, P. Calabrese, and F. H. L. Essler, *SciPost Phys.* **1**, 001 (2016).
- [18] E. H. Lieb and W. Liniger, *Phys. Rev.* **130**, 1605 (1963).
- [19] T. Kinoshita, T. Wenger, and D. S. Weiss, *Science* **305**, 1125 (2004).
- [20] B. Paredes, A. Widera, V. Murg, O. Mandel, S. Fölling, I. Cirac, G. V. Shlyapnikov, T. W. Hänsch, and I. Bloch, *Nature* **429**, 277 (2004).
- [21] E. Haller, M. Gustavsson, M. J. Mark, J. G. Danzl, R. Hart, G. Pupillo, and H.-C. Nägerl, *Science* **325**, 1224 (2009).
- [22] M. Girardeau, *Journal of Mathematical Physics* **1**, 516 (1960).
- [23] M. D. Girardeau, *Phys. Rev.* **139**, B500 (1965).
- [24] M. D. Girardeau and E. M. Wright, *Phys. Rev. Lett.* **84**, 5239 (2000).
- [25] V. Yukalov and M. Girardeau, *Laser Physics Letters* **2**, 375 (2005).
- [26] A. Minguzzi and D. M. Gangardt, *Phys. Rev. Lett.* **94**, 240404 (2005).
- [27] R. Pezer and H. Buljan, *Phys. Rev. Lett.* **98**, 240403 (2007).
- [28] M. Collura, S. Sotiriadis, and P. Calabrese, *Phys. Rev. Lett.* **110**, 245301 (2013).
- [29] E. Quinn and M. Haque, *Phys. Rev. A* **90**, 053609 (2014).
- [30] A. S. Campbell, D. M. Gangardt, and K. V. Kheruntsyan, *Phys. Rev. Lett.* **114**, 125302 (2015).
- [31] R. Van den Berg, B. Wouters, S. Eliëns, J. De Nardis, R. M. Konik, and J.-S. Caux, *Phys. Rev. Lett.* **116**, 225302 (2016).
- [32] A. Lenard, *Journal of Mathematical Physics* **7**, 1268 (1966).
- [33] P. Vignolo and A. Minguzzi, *Phys. Rev. Lett.* **110**, 020403 (2013).
- [34] Y. Hao, Y. Song, and X. Fu, *International Journal of Modern Physics B* **30**, 1650216 (2016).
- [35] I. Bouchoule, S. S. Szigeti, M. J. Davis, and K. V. Kheruntsyan, *Phys. Rev. A* **94**, 051602 (2016).
- [36] Y. Y. Atas, I. Bouchoule, D. M. Gangardt, and K. V. Kheruntsyan, [arXiv:1612.04593](https://arxiv.org/abs/1612.04593).
- [37] S. Wu, Y.-J. Wang, Q. Diot, and M. Prentiss, *Phys. Rev. A* **71**, 043602 (2005).
- [38] Y. Y. Atas, I. Bouchoule, D. M. Gangardt, and K. V. Kheruntsyan, in preparation.
- [39] H. Buljan, R. Pezer, and T. Gasenzer, *Phys. Rev. Lett.* **100**, 080406 (2008).
- [40] See the Supplemental Material at <http://link.aps.org/> supplemental/XXX, which contains additional details on Lenard's formula and the derivation of Eq. (6).
- [41] P. Forrester, N. Frankel, T. Garoni, and N. Witte, *Communications in Mathematical Physics* **238**, 257 (2003).
- [42] M. Jimbo, T. Miwa, Y. Môri, and M. Sato, *Physica D: Nonlinear Phenomena* **1**, 80 (1980).
- [43] A. Perelomov and Y. Zel'dovich, *Quantum Mechanics* (World Scientific, Singapore, 1998).
- [44] J. C. Piquette, *Journal of Symbolic Computation* **11**, 231 (1991).

## Supplemental Material: Exact nonequilibrium dynamics of finite-temperature Tonks-Girardeau gases

Y. Y. Atas,<sup>1</sup> D. M. Gangardt,<sup>2</sup> I. Bouchoule,<sup>3</sup> and K. V. Kheruntsyan<sup>1</sup>

<sup>1</sup>*University of Queensland, School of Mathematics and Physics, Brisbane, Queensland 4072, Australia*

<sup>2</sup>*School of Physics and Astronomy, University of Birmingham, Edgbaston, Birmingham, B15 2TT, UK*

<sup>3</sup>*Laboratoire Charles Fabry, Institut d'Optique, CNRS, Université Paris Sud 11,*

*2 Avenue Augustin Fresnel, F-91127 Palaiseau Cedex, France*

(Dated: December 14, 2016)

### ONE-BODY DENSITY MATRIX FROM THE FREDHOLM DETERMINANT APPROACH

According to Lenard's formula [1, 2], the finite-temperature one-body density matrix  $\rho(x, y; t)$  of the TG gas can be expressed as an infinite series

$$\begin{aligned} \rho(x, y; t) = & \sum_{j=0}^{\infty} \frac{(-2)^j}{j!} [\text{sign}(x - y)]^j \\ & \times \int_x^y dx_2 \cdots dx_{j+1} \det_{k,l=1}^{j+1} [\rho_F(x_k, x_l; t)], \end{aligned} \quad (\text{S1})$$

where

$$\rho_F(x, y; t) = \sum_{i=0}^{\infty} f_i \phi_i(x, t) \phi_i^*(y, t) \quad (\text{S2})$$

is the fermionic one-body density matrix,  $f_i = [e^{(E_i - \mu)/k_B T_0} + 1]^{-1}$  is the Fermi-Dirac occupation factor of the  $i$ th single-particle orbital ( $i = 0, 1, \dots$ ) of energy  $E_i$ , and in the determinant in Eq. (S1) one has to take  $x_k = x$  for  $k = 1$  and  $x_l = y$  for  $l = 1$ ; the  $j = 0$  term in the sum is given by  $\rho_F(x, y; t)$  itself. In practice, it is difficult to use this formula for increasingly higher  $j$  (for example, in Ref. [2] only  $j \leq 3$  terms were included in the calculated examples) as the large- $j$  terms contain multiple ( $j$ -fold) integrals, in addition to entering the sum with alternating signs that lead to numerical inaccuracies.

As we mentioned in the main text, while previous work on finite-temperature TG gases relied on the above Lenard's formula for calculating  $\rho(x, y; 0)$  (see, e.g., [2, 3]), here we develop a method that is based on the Fredholm determinant approach, represented by Eqs. (4)-(5) of the main text. We point out that Eq. (S1) corresponds to the expansion of the determinant in Eq. (4) by minors [4, 5], and that a discrete version of Eq. (4) on the lattice has previously been obtained by Y. Castin for a spatially homogeneous TG gas at  $T = 0$  (see Eq. (3.37) in [6]).

At zero temperatures, the infinite sum appearing in the fermionic one-body density matrix (S2), which also serves the role of the kernel  $K$  in Eq. (5) of the main text, is effectively truncated by the highest occupied orbital term ( $i = N - 1$ ) corresponding to the Fermi level. At finite temperatures this is no longer true; however, for any practical calculation the infinite series can be truncated at some large  $M$  beyond which

the Fermi-Dirac occupancies are negligible. (In practice, the precise value of the cutoff  $M$  should be determined from the convergence properties of the final physical results of interest.) Therefore, to a good approximation, the fermionic kernel in Eq. (5) of the main text can be replaced by a finite series  $\rho_F(w, r; t) \simeq K_M(w, r; t) = \sum_{i=0}^M f_i \phi_i(w, t) \phi_i^*(r, t)$ . Inserting this form of the kernel into Eq. (5) gives

$$R(u, v; t) = K_M(u, v; t) + 2 \sum_{i=0}^M \sqrt{f_i} \phi_i(u, t) A_i(v; t), \quad (\text{S3})$$

where we have introduced the following notation,

$$A_i(v; t) = \sqrt{f_i} \int_x^y \phi_i^*(r, t) R(r, v; t) dr. \quad (\text{S4})$$

The functions  $A_i(v; t)$  are determined as follows. Multiplying Eq. (S3) by  $\sqrt{f_j} \phi_j^*(u, t)$  and integrating on  $[x, y]$ , we obtain

$$A_j(v; t) = \sum_{i=0}^M S_{ji}(t) \left[ \sqrt{f_i} \phi_i^*(v) + 2A_i(v) \right], \quad (\text{S5})$$

where the matrix elements  $S_{ij} = (\mathbf{S})_{ij}$  are given by

$$S_{ij}(t) = \text{sign}(y - x) \sqrt{f_i f_j} \int_x^y \phi_i^*(x', t) \phi_j(x', t) dx', \quad (\text{S6})$$

and where we again suppressed the dependence of  $S_{ij}(t)$  on the integration limits.

We proceed by writing the equation satisfied by the functions  $A_i$  in a more compact matrix form. By writing the left hand side of Eq. (S5) as  $A_j(v; t) = \sum_{i=0}^M \delta_{ji} A_i(v; t)$  we obtain

$$\sum_{i=0}^M [\delta_{ji} - 2S_{ji}(t)] A_i(v; t) = \sum_{i=0}^M S_{ji}(t) \sqrt{f_i} \phi_i^*(v, t). \quad (\text{S7})$$

Introducing the vectors  $\vec{A} = (A_0, \dots, A_M)^\top$  and  $\vec{\Phi} = (\sqrt{f_0} \phi_0^*, \dots, \sqrt{f_M} \phi_M^*)^\top$ , this can be rewritten as a matrix equation  $[\mathbb{1} - 2\mathbf{S}(t)] \vec{A}(v; t) = \mathbf{S}(t) \vec{\Phi}(v, t)$ , which in turn can be inverted to yield  $\vec{A}(v; t) = [\mathbb{1} - 2\mathbf{S}(t)]^{-1} \mathbf{S}(t) \vec{\Phi}(v, t)$ . Inserting this expression into Eq. (S3) and rewriting the fermionic kernel as a double sum,  $K_M(u, v; t) =$

$\sum_{i,j} [\sqrt{f_i} \phi_i(u, t) \delta_{ij} \sqrt{f_j} \phi_j^*(v, t)]$ , we obtain that the resolvent operator  $R(x, y; t)$  is given by

$$R(x, y; t) = \sum_{i,j=0}^M \sqrt{f_i} \phi_i(x, t) (\mathbb{1} - 2\mathbf{S}^{-1})_{ij} \sqrt{f_j} \phi_j^*(y, t). \quad (\text{S8})$$

The Fredholm determinant that appears in the definition of the one-body density matrix, Eq. (4) of the main text, is equal to  $\det(\mathbb{1} - 2\mathbf{S})$  in the truncated basis [4] and therefore the corresponding final expression for the one-body density matrix of TG gas at finite temperature can be written as

$$\rho(x, y; t) = \sum_{i,j=0}^M \sqrt{f_i} \phi_i(x, t) Q_{ij}(x, y; t) \sqrt{f_j} \phi_j^*(y, t). \quad (\text{S9})$$

Here, the  $M \times M$  matrix  $\mathbf{Q}$ , with elements  $Q_{ij}(x, y; t)$ , is given by  $\mathbf{Q} = (\mathbf{P}^{-1})^\top \det \mathbf{P}$ , where the matrix elements of  $\mathbf{P}$  are determined from

$$P_{ij}(x, y; t) = \delta_{ij} - 2 \operatorname{sgn}(y - x) \sqrt{f_i f_j} \int_x^y dx' \phi_i(x', t) \phi_j^*(x', t). \quad (\text{S10})$$

In the limit  $M \rightarrow \infty$ , Eq. (S9) becomes equivalent to Eq. (6) of the main text.

---

- [1] A. Lenard, *Journal of Mathematical Physics* **7**, 1268 (1966).
- [2] P. Vignolo and A. Minguzzi, *Phys. Rev. Lett.* **110**, 020403 (2013).
- [3] Y. Hao, Y. Song, and X. Fu, *International Journal of Modern Physics B* **30**, 1650216 (2016).
- [4] F. Bornemann, *Mathematics of Computation* **79**, 871 (2010).
- [5] P. Forrester, N. Frankel, T. Garoni, and N. Witte, *Communications in Mathematical Physics* **238**, 257 (2003).
- [6] Y. Castin, *Journal de Physique IV* **116**, 89 (2004).